



| | |
|------------------------------------|---|
| Title | The surface-associated exopolysaccharide of <i>Bifidobacterium longum</i> 35624 plays an essential role in dampening host proinflammatory responses and repressing local TH17 responses |
| Author(s) | Schiavi, Elisa; Gleinser, Marita; Molloy, Evelyn; Groeger, David; Frei, Remo; Ferstl, Ruth; Rodriguez-Perez, Noelia; Ziegler, Mario; Grant, Ray; Moriarty, Thomas Fintan; Plattner, Stephan; Healy, Selena; O'Connell Motherway, Mary; Akdis, Cezmi A.; Roper, Jennifer; Altmann, Friedrich; van Sinderen, Douwe; O'Mahony, Liam |
| Publication date | 2016-12 |
| Original citation | Schiavi, E., Gleinser, M., Molloy, E., Groeger, D., Frei, R., Ferstl, R., Rodriguez-Perez, N., Ziegler, M., Grant, R., Moriarty, T. F., Plattner, S., Healy, S., O'Connell Motherway, M., Akdis, C. A., Roper, J., Altmann, F., van Sinderen, D. and O'Mahony, L. (2016) 'The Surface-Associated Exopolysaccharide of <i>Bifidobacterium longum</i> 35624 Plays an Essential Role in Dampening Host Proinflammatory Responses and Repressing Local TH17 Responses', <i>Applied and Environmental Microbiology</i> , 82(24), pp. 7185-7196. doi:10.1128/aem.02238-16 |
| Type of publication | Article (peer-reviewed) |
| Link to publisher's version | http://aem.asm.org/content/82/24/7185.abstract http://dx.doi.org/10.1128/aem.02238-16 Access to the full text of the published version may require a subscription. |
| Rights | © 2016, American Society for Microbiology. All Rights Reserved. |
| Item downloaded from | http://hdl.handle.net/10468/5413 |

Downloaded on 2018-08-23T19:27:56Z

1 The surface associated exopolysaccharide of *Bifidobacterium longum* 35624 plays an essential role in
2 dampening host pro-inflammatory responses and in repressing local TH17 responses

3 **Running title:** *B. longum* exopolysaccharide modulates TH17 responses

4 Elisa Schiavi^{a,b}, Marita Gleinser^c, Evelyn Molloy^c, David Groeger^b, Remo Frei^a, Ruth Ferstl^a,
5 Noelia Rodriguez-Perez^a, Mario Ziegler^a, Ray Grant^b, Thomas Fintan Moriarty^d, Stephan
6 Plattner^e, Selena Healy^e, Mary O'Connell Motherway^c, Cezmi A. Akdis^a, Jennifer Roper^e,
7 Friedrich Altmann^f, Douwe van Sinderen^c, Liam O'Mahony^{a#}

8 ^aSwiss Institute of Allergy and Asthma Research (SIAF), University of Zürich, Davos,
9 Switzerland; ^bAlimentary Health Pharma Davos, Davos, Switzerland; ^cAPC Microbiome
10 Institute and School of Microbiology, University College Cork, Cork, Ireland; ^dAO Research
11 Institute Davos, Davos, Switzerland; ^eAlimentary Health, Cork Ireland; ^fBOKU, Vienna,
12 Austria

13 Running Head: Immunoregulation by bifidobacterial surface polysaccharide

14

15 #Address correspondence to Liam O'Mahony, liam.omahony@siaf.uzh.ch.

16

17 Abstract word count: 200

18 Manuscript word count: 5,926

19 **ABSTRACT**

20 The immune modulating properties of certain bifidobacterial strains, such as *Bifidobacterium*
21 *longum* subsp. *longum* **35624**TM (*B. longum* 35624), have been well described, although the
22 strain-specific molecular characteristics associated with such immune regulatory activity are
23 not well defined. It has previously been demonstrated that *B. longum* **35624** produces a cell
24 surface exopolysaccharide and in this study we investigated the role played by this
25 exopolysaccharide in influencing the host immune response. *B. longum* **35624** induced
26 relatively low levels of cytokine secretion from human dendritic cells, whereas an isogenic
27 exopolysaccharide-negative mutant derivative (termed sEPS^{neg}) induced vastly more
28 cytokines, including IL-17, which was reversed when exopolysaccharide production was
29 restored in sEPS^{neg} by genetic complementation. Administration of *B. longum* **35624** to the T
30 cell transfer colitis model prevented disease symptoms, whereas sEPS^{neg} did not protect
31 against the development of colitis, with associated enhanced recruitment of IL-17+
32 lymphocytes to the gut. Moreover, intra-nasal administration of sEPS^{neg} also resulted in
33 enhanced recruitment of IL-17+ lymphocytes to the murine lung. These data demonstrate that
34 the particular exopolysaccharide produced by *B. longum* **35624** plays an essential role in
35 dampening pro-inflammatory host responses to the strain and that loss of exopolysaccharide
36 production results in the induction of local T_H17 responses.

37 **IMPORTANCE**

38 Particular gut commensals, such as *B. longum* **35624**, are known to contribute positively to
39 the development of mucosal immune cells, resulting in protection from inflammatory
40 diseases. However, the molecular basis and mechanisms for these commensal-host
41 interactions are poorly described. In this report, an exopolysaccharide was shown to be

42 decisive in influencing the immune response to the bacterium. We generated an isogenic
43 mutant unable to produce exopolysaccharide, and observed that this mutation caused a
44 dramatic change in the response of human immune cells *in vitro*. In addition, mouse models
45 confirmed that lack of exopolysaccharide production induces inflammatory responses to the
46 bacterium. These results implicate the surface-associated exopolysaccharide of the *B. longum*
47 **35624** cell envelope in the prevention of aberrant inflammatory responses.
48

49 INTRODUCTION

50 The gut microbiota contributes significantly to host health via multiple mechanisms,
51 including the digestion of foods, competitive exclusion of pathogens, enhancement of
52 epithelial cell differentiation and promotion of mucosa-associated lymphoid tissue
53 proliferation (1, 2). Furthermore, accumulating evidence suggests that the composition and
54 metabolic activity of the gut microbiota has profound effects on proinflammatory activity and
55 the induction of immune tolerance within mucosal tissue (3-5). Certain microbes induce
56 regulatory responses, while others induce effector responses, resulting in the case of healthy
57 individuals in a balanced homeostatic immunological state, which protects against infection
58 and controls aberrant, tissue-damaging inflammatory responses (6).

59 One bacterial strain, which is known to induce tolerogenic responses within the gut, is
60 *Bifidobacterium longum* subsp. *longum* **35624**TM (7). Induction of T regulatory (Treg) cells by
61 the *B. longum* **35624** strain in mice is associated with protection against colitis, arthritis,
62 allergic responses and pathogen-associated inflammation (8-12). Administration of this
63 bacterium to humans increases Foxp3⁺ lymphocytes in peripheral blood, enhances IL-10
64 secretion *ex vivo*, and reduces the level of circulating proinflammatory biomarkers in a wide
65 range of patient groups (13, 14). A number of host mechanisms have been described, which
66 contribute to the anti-inflammatory activity of this microbe, including Toll-like receptor 2
67 (TLR-2) and Dendritic Cell-Specific Intercellular adhesion molecule-3-Grabbing Non-
68 integrin (DC-SIGN) recognition, and retinoic acid release by dendritic cells (13, 15-17).
69 However, the bacterial strain-specific structural and/or metabolic factors that contribute to
70 these protective immune responses have as yet remained elusive.

71 A number of different exopolysaccharides from gut microbes have been shown to
72 induce immune-modulatory effects. Polysaccharide A (PSA) from *Bacteroides fragilis*
73 mediates the conversion of naïve CD4⁺ T cells into Foxp3⁺ Treg cells that produce IL-10
74 during commensal colonization. Functional Treg cells are also induced by PSA during
75 intestinal inflammation, which requires TLR-2 signaling (18). Further studies have reported
76 that PSA interacts directly with mouse plasmacytoid dendritic cells via TLR-2 and that PSA-
77 exposed plasmacytoid dendritic cells express molecules involved in protection against colitis
78 and stimulate CD4⁺ T cells to secrete IL-10 (19). An exopolysaccharide from *Bacillus subtilis*
79 prevents gut inflammation stimulated by *Citrobacter rodentium*, which is dependent on TLR-
80 4 and MyD88 signaling (20). Similarly, protection against *C. rodentium* infection by
81 *Bifidobacterium breve* UCC2003 was dependent on the presence of its exopolysaccharide
82 (21). Furthermore, it was described that an extracellular polymeric matrix, isolated from
83 *Faecalibacterium prausnitzii*, displayed anti-inflammatory activity in the mouse dextran
84 sodium sulphate colitis model (22).

85 We recently described that the *B. longum* **35624** strain-specific EPS gene cluster,
86 designated as *eps_{624s}* is responsible for the production of a cell surface-associated
87 exopolysaccharide, composed of a branched hexasaccharide repeating unit with two
88 galactoses, two glucoses, galacturonic acid and the unusual sugar 6-deoxytalose (23). The
89 overall aim of the current study was to determine if the exopolysaccharide produced by *B.*
90 *longum* **35624** is related with the immunoregulatory effects of this microorganism. To address
91 this aim, we investigated if an isogenic derivative of *B. longum* **35624**, which does not
92 produce exopolysaccharide, is able to exert similar immunological effects to its parent strain
93 *in vitro* and in colitis and asthma mouse models.

94

95 **MATERIALS AND METHODS**

96 **Bacterial strains, plasmids and culture conditions.** Bacterial strains and plasmids used in
97 this study are detailed in Table 1. Bifidobacteria were routinely cultured in either de Man
98 Rogosa and Sharpe medium (MRS; Oxoid Ltd., Basingstoke, Hampshire, United Kingdom)
99 supplemented with 0.05 % cysteine-HCl or reinforced clostridial medium (RCM; Oxoid Ltd.).
100 Bifidobacterial cultures were incubated at 37 °C under anaerobic conditions in a Don Whitley
101 anaerobic Chamber. *Escherichia coli* strains were cultured in Lysogeny broth (LB; Oxoid
102 Ltd) at 37 °C with agitation. Where appropriate, growth media contained chloramphenicol
103 (Cm; 10 µg ml⁻¹ for *E. coli* and 5 µg ml⁻¹ for *B. longum* **35624**), erythromycin (Em; 100 µg
104 ml⁻¹ for *E. coli*), tetracycline (Tet; 10 µg ml⁻¹ for *E. coli* and 10 µg ml⁻¹ for *B. longum* **35624**),
105 ampicillin (Amp; 100 µg ml⁻¹ for *E. coli*) or kanamycin (Km; 50 µg ml⁻¹ for *E. coli*). All
106 antibiotics were obtained from Sigma Aldrich, Dorset, England). The commercially available
107 *B. longum* **35624**TM culture was provided by Alimentary Health limited (Cork, Ireland).

108 **DNA manipulations.** Chromosomal DNA was isolated from bifidobacteria as
109 previously described (24). Minipreparation of plasmid DNA from *E. coli* or *B. longum* **35624**
110 was achieved using the Qiaprep spin plasmid miniprep kit (Qiagen GmbH, Hilden,
111 Germany). For *B. longum* **35624** an initial lysis step was incorporated into the plasmid
112 isolation procedure, cells were resuspended in lysis buffer supplemented with lysozyme (30
113 mg ml⁻¹) and incubated at 37 °C for 30 min. Restriction enzymes and T4 DNA ligase were
114 used according to the supplier's instructions (Roche Diagnostics, Bell Lane, East Sussex,
115 UK). Synthetic single stranded oligonucleotide primers used in this study were obtained from
116 Eurofins (Ebersberg, Germany) and are detailed in Table 2. Standard PCRs were performed

6

117 using TaqPCR mastermix (Qiagen), while high fidelity PCR was achieved using *PfuII*
118 polymerase (Agilent, Santa Clara, California). *B. longum* **35624** colony PCRs were performed
119 according to standard procedures with the addition of an initial incubation step of 95 °C for 5
120 minutes to perform cell lysis. PCR fragments were purified using the Qiagen PCR purification
121 kit. Following electroporation of plasmid DNA into *E.coli* strain EC101,
122 electrotransformation of *B. longum* **35624** or sEPS^{neg} was performed essentially as described
123 by Maze *et al.* (25) with the following modifications. An overnight culture of *B. longum*
124 **35624** was sub-cultured twice (first using a 2 % inoculum and then a 1 % inoculum) in MRS
125 supplemented with 0.05 % cysteine-HCl and 0.2 M sucrose prior to inoculating (4%)
126 modified Rogosa medium supplemented with 0.05 % cysteine-HCl, 1% (w/v) glucose and 0.2
127 M sucrose. Bacteria were grown until the OD₆₀₀ had reached 0.3-0.4, after which cells were
128 harvested by centrifugation (6,500 rpm, 10 min, and 4 °C) and washed twice using 1 mM
129 ammonium citrate buffer (pH 6.0) supplemented with 0.5 M sucrose. An additional
130 centrifugation step (9,800 *g, 10 min, and 4 °C) was included to concentrate the competent
131 cells. For electroporation 5 µl of plasmid DNA was mixed with 50 µl of competent cells,
132 transferred into an electroporation cuvette with 0.2 cm inter-electrode distance and pulsed at
133 2.5 kV, 25 µF and 200 Ω using a Gene Pulser II Electroporation System (Biorad, Hercules,
134 California USA). For recovery, 800 µl of RCM supplemented with 0.05 % L-cysteine
135 hydrochloride were added to bacteria and incubated anaerobically for 2.5 h at 37 °C.
136 Transformations were plated on reinforced clostridial agar (RCA) plates supplemented with
137 appropriate concentrations of relevant antibiotics and incubated 2-3 days anaerobically at 37
138 °C. The correct orientation and integrity of all constructs was verified by PCR and subsequent
139 DNA sequencing, which was performed at Eurofins (Ebersberg, Germany).

140 **Construction of sEPS^{neg}**. An internal 583 bp fragments of the *pgt₆₂₄* gene was
141 amplified by PCR using *B. longum* **35624** chromosomal DNA as a template and the
142 oligonucleotide primers *BI0342F_HindIII* and *BI0342R_XbaI*. The PCR product generated
143 was ligated to pORI19, an Ori⁺ RepA- integration plasmid (26), using the unique *HindIII* and
144 *XbaI* restriction sites that were incorporated into the primers for the *pgt* fragment-
145 encompassing amplicon, and introduced into *E. coli* EC101 by electroporation. Recombinant
146 *E. coli* EC101 derivatives containing pORI19 constructs were selected on LB agar containing
147 Em, and supplemented with X-gal (5-bromo-4-chloro-3-indolyl- β -D-galactopyranoside) (40
148 $\mu\text{g ml}^{-1}$) and IPTG (isopropyl- β -D galactopyranoside) (1 mM). The expected genetic structure
149 of the recombinant plasmid, designated pORI19-*pgt*, was confirmed by restriction mapping
150 prior to subcloning of the Tet resistance antibiotic cassette, *tet(W)*, from pAM5 (27) as a *SacI*
151 fragment into the unique *SacI* site on pORI19-*pgt*. The expected structure of a single
152 representative of the resulting plasmid, designated pORI19*tet(W)*-*pgt*, was confirmed by
153 restriction analysis. The plasmid was introduced into *E. coli* EC101 harbouring pNZ-M.1185
154 (this is a plasmid expressing a *B. longum* **35624**-encoded methylase) by electroporation, and
155 transformants were selected based on Em and Tet resistance. Methylation of the resulting
156 plasmid complement of such transformants by the *M.1185* (isoschizomer of *M.EcoRII*) was
157 confirmed by their observed resistance to *EcoRII* restriction. Plasmid preparations of
158 methylated pORI19*tet(W)*-*pgt* were introduced by electroporation into *B. longum* **35624** with
159 subsequent selection on RCA plates supplemented with Tet.

160 **Construction of sEPS^{comp}**. For the construction of plasmid pBC1.2-*pgt₆₂₄* +*BI0343*, a
161 DNA fragment encompassing *pgt₆₂₄* plus the downstream located gene with locus tag BI0343
162 and the presumed promoter region was generated by PCR amplification from chromosomal

163 DNA of *B. longum* **35624** using *PfuII* polymerase and primer combinations BI0342FSalI and
164 BI0343EcoRI, where *SalI* or *EcoRI* restriction sites were incorporated at the 5' ends of the
165 forward primer, and reverse primer, respectively. Amplicons were digested with *SalI*, and
166 *EcoRI*, and ligated into similarly digested pBC1.2 prior to introduction into *E. coli* XL1blue
167 by electroporation and subsequent selection of transformants on LB agar supplemented with
168 Tet and Amp. The integrity of positive clones was confirmed by sequencing and one selected
169 clone designated pBC1.2 *pgt+BI0343* was introduced into sEPS^{neg} by electroporation with
170 subsequent selection of transformants on RCA supplemented with Tet and Cm. The resultant
171 sEPS^{neg} strain harboring pBC1.2 *pgt+BI0343* was designated sEPS^{comp}.

172 **Electron Microscopy.** After culture in MRS medium, bacteria were gently rinsed in
173 Piperazine-N,N-bis-2-ethane sulphonic acid (PIPES) buffer (0.1 M, pH 7.4) before being
174 fixed in 2.5 % glutaraldehyde in PIPES buffer for 5 min. The samples were rinsed twice (2
175 min each time) in PIPES buffer and post-fixed with 1 % osmium tetroxide in 0.1 M PIPES
176 buffer (pH 6.8), for 60 min in the dark. The samples were rinsed three times in double
177 distilled water (2 min each wash) before dehydration through an ethanol series (50, 70, 96,
178 and 100 %) for 5 min each. All fixation and washing steps were carried out at room
179 temperature. Following dehydration, the samples were critically point dried in a POLARON
180 E3100 critical point drier (Agar Scientific, Stansted, UK), and coated with 10 nm of
181 gold/palladium (80/20) using a Baltec MED 020 unit (Baltec, Buchs, Liechtenstein). Bacterial
182 preparations were examined using a Hitachi S-4700 scanning electron microscope (SEM),
183 operated in secondary electron detection mode (3 kV, 40 μ A) and images captured with
184 Quartz PCI (Quartz Imaging Corporation, Vancouver, Canada).

185 **Exopolysaccharide isolation.** The exopolysaccharide was isolated as previously
186 described (23). Briefly, following harvesting of *B. longum* **35624** cells, which were grown on
187 agar plates to minimize carryover of media components, an exopolysaccharide solution was
188 generated by agitating the cells in PBS. The harvested exopolysaccharide solution was mixed
189 with ethanol and the exopolysaccharide aggregated at the center of the surface of the ethanol
190 solution, which facilitated harvesting of the exopolysaccharide without the need for
191 centrifugation. The exopolysaccharide aggregations were taken with a spatula, resuspended in
192 water and dialysed against water to remove contaminants and residual ethanol. The
193 exopolysaccharide was applied 2 times on Bakerbond SPE C18 columns (Avantor, Deventer,
194 The Netherlands) as indicated by the manufacturer using a HyperSep-96™ vacuum manifold
195 (Thermo Scientific, Waltham, USA). The flow-through fraction was collected and filtered
196 through 0.45 µm syringe filters. Quantification of total carbohydrate levels was performed as
197 previously described (28) using a phenol-sulphuric acid method in microplate format. The
198 absence of contaminating proteins was confirmed by measuring the total soluble protein
199 content of the exopolysaccharide preparation using the BCA protein quantification kit
200 (Thermo Scientific) according to manufacturer's instructions. Bovine serum albumin was
201 used for generation of standards. Lipopolysaccharide contamination was monitored using the
202 pyrogene recombinant factor C assay (Lonza, Bettlach, Switzerland).

203 ***In vitro* immune assays.** Human blood was purchased from the Swiss blood bank
204 (Blutspendezentrum, Basel, Switzerland), which obtains the blood following appropriate
205 screening and consenting of volunteers. Blood samples were anonymized and coded prior to
206 leaving the blood bank. Research procedures on human blood were performed in accordance
207 with Swiss law (ethical approval number KEK Nr. 19/08). All experiments with human
208 blood-derived cells were conducted under biosafety level 2 conditions. Peripheral blood
10

209 mononuclear cells (PBMCs) were isolated from healthy donors using density gradient
210 centrifugation. Human monocyte-derived dendritic cells (MDDCs) were differentiated with
211 1000 IU ml⁻¹ GM-CSF (Peprotech, London, UK) and 1000 IU ml⁻¹ IL-4 (Novartis, Basel,
212 Switzerland) from purified CD14⁺ cells using MACS separation (Miltenyi Biotec, Bergisch
213 Gladbach, Germany). Bacterial strains for *in vitro* assays were cultured in MRS medium
214 supplemented with 0.05 % L-cysteine for 48 hours under anaerobic conditions at 37°C. Cells
215 were harvested and washed once with sterile PBS by centrifugation at 6,500 rpm for 10
216 minutes. Bacterial cell number was determined by microscopy using a Petroff-Hausser
217 chamber and bacteria were diluted as appropriate in PBS for incubation with human cells.
218 PBMCs and MDDCs were stimulated for 24 h at 37°C, 5 % CO₂ with bacterial strains at a
219 concentration of 50 bacterial cells to 1 PBMC or MDDC. Human and bacterial cell co-
220 cultures were performed in complete RPMI-1640 (cRPMI) medium (Sigma, Buchs,
221 Switzerland) supplemented with 10% fetal bovine serum (Sigma), penicillin (100 Units ml⁻¹)
222 and streptomycin (0.1 mg ml⁻¹) (Sigma). Purified exopolysaccharide from *B. longum* **35624**
223 was also added (final concentration 100 µg/ml) to PBMC cultures (in duplicate) stimulated
224 with sEPS^{neg}. Cytokine concentrations were measured using the Bio-Plex Multiplex System
225 (Biorad). For human dendritic cells staining, the following antibodies were used: PE-Cy7
226 anti-human CD274 (PD-L1), APC anti-human CD273 (PD-L2) and Pacific Blue anti-human
227 CD11c (eBioscience, Vienna, Austria). THP-1-BlueTM NF-κB monocyte cell line (Invivogen,
228 San Diego, USA) was maintained and sub-cultured in cRPMI medium (Sigma) in presence of
229 200µg/ml Zeocin (Invivogen). For the co-culture experiment with bacteria, 10⁵ cells/well
230 were seeded in a 96 well-plate in a total volume of 200 µl/well of cRPMI medium. The cells
231 were stimulated over a range of different bacterial concentrations for 24 h and activation of
232 NF-κB/AP-1 pathway was evaluated by Quanti-BlueTM assay according to the manufacturer's

11

233 instructions. In addition, MDDCs were stimulated with different bacterial strains and NF- κ B
234 phosphorylation measured over a time course. MDDCs were lysed using Bio-Plex Pro cell
235 signaling reagent kit (Biorad) and cell lysates were stored at -80°C until analysis. Protein
236 concentration was determined using Bio-Rad's DC™ protein assay and equal amounts of
237 protein were used to measure NF- κ B p65 (Ser⁵³⁶) in the Bio-Plex Pro™ Magnetic Cell
238 Signaling Assay (Biorad). Results are expressed as MFI (mean fluorescence intensity).

239 **T cell transfer colitis model.** C.B-17 severe combined immunodeficient (SCID and
240 BALB/c female mice (8-12 weeks of age) were obtained from Charles River (Sulzfeld,
241 Germany) and maintained under specific pathogen free conditions. The animals were housed
242 at the AO Research Institute, Davos, Switzerland, in individually ventilated cages for the
243 duration of the study, and all experimental procedures were carried out in accordance with
244 Swiss law (Permit number: 2013_32). Colitogenic CD4⁺CD25⁻CD45RB^{hi} cells were isolated
245 from BALB/c donor mouse spleens using the MACS Miltenyi system (depletion of
246 CD4⁺CD25⁺ cells followed by positive selection of CD45RB FITC-labeled cells). At day 0,
247 colitis was induced by intraperitoneal transfer of 4×10^5 cells per C.B-17 SCID mouse (8
248 mice per group). Bacterial cells were prepared as described above and counted using
249 microscopy (Petroff-Hausser chamber) prior to dilution in sterile PBS. 1×10^9 *B. longum*
250 **35624** cells, or its isogenic derivatives, were administered to each mouse by intragastric
251 gavage (total volume of 200 μ l). Bacteria were gavaged from the beginning of the study (day
252 0) and continued to be gavaged every second day until animals were euthanized at the end of
253 the study. Sixteen days after study initiation, disease severity scores were recorded, while
254 animal weights were monitored every day. Disease severity scores included feces condition (
255 1 - wet; 2 - diarrhea; 3 - bloody diarrhea or rectal prolapse), activity (1 - isolated, abnormal

256 position; 2 - huddled, hypoactive or hyperactive; 3 – unconscious), coordination of movement
257 (1 - slightly uncoordinated; 2 – very uncoordinated; 3 – paralysis) and fur quality (1 – reduced
258 grooming; 2 – disheveled; 3 - hair loss). Gut transit was determined by quantifying fecal *B.*
259 *longum* **35624** levels by PCR. *B. longum* **35624** specific primers were designed using Primer3
260 software (<http://simgene.com/Primer3>). The primers, designated 2420t (Forward: CAG TGG
261 GGT GCG ACT ACA; Reverse: GCG CGA ACC AGA AGA TGT) generated a 494 bp
262 amplicon. Bacterial DNA from fecal samples was extracted using QIAamp DNA Stool Mini
263 Kit (Qiagen). DNA was quantified using Nanodrop (Thermo Scientific) and 100 ng of total
264 DNA was assayed using SYBR Green PCR Master Mix (Biorad). The thermal cycling
265 conditions consisted of an initial denaturation step of 15 min at 95°C, followed by 30 cycles
266 of denaturation at 94°C for 45 sec, annealing for 45 sec at 56°C, and extension at 72°C for 45
267 sec. *B. longum* **35624** DNA concentrations were quantified using the absolute quantitation
268 protocol of the ABI 7900 Fast real-Time PCR system (Applied Biosystem, CA, USA). In a
269 parallel experiment, BALB/c healthy mice (6 mice per group) were gavaged with *B. longum*
270 **35624** or its isogenic derivative for 3 weeks, as described above for the colitis study.

271 Following euthanasia on day 26, mesenteric lymph nodes were isolated in order to
272 obtain single cell suspensions. Lymph nodes were mechanically disrupted using a syringe
273 plunger to grind the nodes on a nylon cell strainer (70 µm). The strainer was washed with
274 PBS and the single cell suspensions were centrifuged at 300 g for 10 minutes. Cell pellets
275 were resuspended in 1 ml of cRPMI medium (Sigma) and cells were counted using a Scepter
276 Cell Counter (Millipore, Billerica, MA, USA). Cells were diluted to a final density of
277 1×10^6 cells ml⁻¹ in cRPMI and cells were dispensed in propylene tubes to perform FACS
278 staining. Lamina propria mononuclear cells were isolated as described previously (29)
279 following removal of epithelial cells and collagenase VIII/DNaseI (Roche) digestion of the
13

280 tissue. At the end of the process, cells were counted using the Sceptor Cell Counter
281 (Millipore) and diluted to a final concentration of 1×10^6 cells ml^{-1} in cRPMI in propylene
282 FACS staining tubes.

283 **OVA respiratory allergy model.** Female BALB/c mice (8-12 weeks of age) were
284 obtained from Charles River and were maintained under specific pathogen free conditions at
285 the AO Research Institute, Davos, Switzerland, in individually ventilated cages for the
286 duration of the study. All experimental procedures were carried out in accordance with Swiss
287 law (Permit number: 2013_20). 8 mice per group were used in this model. Three
288 intraperitoneal immunizations with 50 μg of ovalbumin (OVA, Grade V>98%, Sigma)
289 emulsified in InjectTM Alum Adjuvant (Life Technologies, Carlsbad, California, USA) were
290 performed on days 0, 14 and 21, followed by OVA aerosol challenges on days 26, 27 and 28.
291 On days 19, 25 and 27, mice received *B. longum* **35624** or sEPS^{neg} intra-nasally ($\sim 1 \times 10^9$
292 bacteria per dose in a total volume of 50 μl of PBS). Bacterial cells were prepared as
293 described above. Control animals received three intraperitoneal injections with Alum adjuvant
294 (without OVA) on days 0, 14 and 21, followed by OVA aerosol challenges on days 26, 27 and
295 28. Control animals also received 50 μl of PBS intra-nasally on days 19, 25 and 27. All mice
296 were sacrificed at day 29 for isolation of lung tissue and flow cytometric staining. Lung-
297 derived single cell suspensions were obtained using a combination of enzymatic digestion
298 (lung dissociation kit, Miltenyi) and mechanical dissociation with a gentleMACS Dissociator
299 (Miltenyi), according to the manufacturer's protocol. Lung cells were plated at 1×10^6 cells/ml
300 in complete RPMI (Sigma) and stimulated *ex vivo* with 50 $\mu\text{g}/\text{ml}$ OVA grade VI (Sigma) or
301 with 500 ng/ml LPS (Sigma) for 48 hours and cytokine secretion quantified by the Bio-Plex
302 Multiplex System (Biorad).

303 **Flow cytometry.** All flow cytometry analyses were performed on the Gallios Flow
304 Cytometer (Beckman Coulter, Brea, USA). Mesenteric lymph node or lung single cell
305 suspensions were stimulated with PMA and ionomycin at 50 ng ml⁻¹ and 500 ng ml⁻¹,
306 respectively, for 4 hours in presence of Brefeldin A (eBioscience). Viability dye eFluor780
307 (eBioscience) and the following surface staining antibodies were used: PE-Cy7 anti-mouse
308 CD3 and Pacific Blue anti-mouse CD4 (Biolegend, San Diego, California USA). Cells were
309 stained for intracellular cytokines using PE anti-mouse IL-10, Alexa Fluor488 anti-mouse/rat
310 IL-17A and PerCP-Cy5.5 anti-mouse IFN- γ after fixation and permeabilization (Intracellular
311 Fixation & Permeabilization Buffer Set, eBioscience). Lamina propria cells were in addition
312 stained for the gut homing molecule CCR9 using Alexa Fluor647 anti-mouse CD199 (CCR9)
313 from Biolegend.

314 **Statistical analysis.** Unless otherwise indicated, data are presented as box-and-
315 whisker plots with the median value and max/min values illustrated. In experiments with
316 technical replicates, the mean was calculated from the technical replicates for each donor and
317 only the mean value was used for the statistical analysis. The Mann–Whitney U test was used
318 for the nonparametric statistical analysis of differences between two groups. For analysis of
319 more than two groups, statistical significance was determined using the Kruskal–Wallis test
320 and Dunn’s multiple comparison test. A two-way ANOVA was used to compare groups over
321 time. A p-value less than 0.05 was considered statistically significant.

322

323 **RESULTS**

324 **Generation of an isogenic exopolysaccharide-negative derivative of *B. longum* 35624,**
325 **designated sEPS^{neg}, by insertion mutagenesis.** In order to determine the role, if any, of the

15

326 exopolysaccharide in the reported immunomodulatory activities of the *B. longum* **35624**
327 strain, we set out to generate an isogenic derivative of this strain that was unable to produce
328 this cell surface-associated glycan exopolymer. For this purpose, we employed a mutagenesis
329 strategy that was based on previously described methods (30). The particular mutagenesis
330 strategy employed for *B. longum* **35624** involved the heterologous expression of a *B. longum*
331 **35624**-encoded DNA methylase in *E. coli* strain EC101 so as to methylate any plasmid DNA
332 in this latter cloning host. When such methylated plasmid DNA is subsequently introduced
333 into *B. longum* **35624**, it will be protected from digestion by the native restriction-
334 modification systems encoded by the latter strain and will therefore allow homology-guided,
335 site-directed mutagenesis as has been described previously (30). Employing this strategy, we
336 created an insertion mutation in the first gene of the *eps*₆₂₄ cluster, i.e. *pgt*₆₂₄, encoding the
337 predicted priming glycosyl transferase (pGT), resulting in an isogenic derivative of *B. longum*
338 **35624**, which was designated sEPS^{neg}.

339 In order to assess if the sEPS^{neg} mutant had, as would be expected, lost its ability to
340 produce exopolysaccharide we performed electron microscopy analysis, which indeed
341 revealed that the ‘stringy’ sEPS layer present on the parent strain *B. longum* **35624** is absent
342 on EPS^{neg}, thus confirming its exopolysaccharide-deficient phenotype (Fig. 1). Furthermore,
343 and in contrast to the parent strain *B. longum* **35624**, the EPS^{neg} strain exhibits a so-called
344 dropping phenotype when grown in liquid medium (i.e. the EPS^{neg} strain was found to
345 sediment during growth in liquid medium, but the *B. longum* **35624** strain remained in
346 suspension). A similar phenotype was observed for exopolysaccharide-negative variants of *B.*
347 *breve* UCC2003 and *Bifidobacterium animalis* subs. *lactis* (21, 31), thereby substantiating the
348 loss of exopolysaccharide production. To ensure that the observed phenotype is directly
349 linked to the inactivation of *pgt*₆₂₄, the adjacent and co-transcribed genes *pgt*₆₂₄ and *BI0343*
16

350 were cloned together with the presumed promoter sequence in plasmid pBC1.2, after which
351 the resultant construct was introduced in the sEPS^{neg} strain. The resulting strain, designated
352 sEPS^{comp}, was shown to produce exopolysaccharide (Fig. 1). A similar complementation
353 approach was previously described (32, 33). The sEPS^{neg} and sEPS^{comp} mutants grew more
354 slowly compared to the parent strain *B. longum* **35624**, likely due to the presence of
355 antibiotics in their culture media, but by 38 hours of culture all bacteria were at similar
356 numbers and had reached stationary phase (Supplementary Fig. S1).

357 ***In vitro* responses to *B. longum* 35624, sEPS^{neg} and sEPS^{comp}.** The wild-type strain
358 *B. longum* **35624** and its derivatives sEPS^{neg} or sEPS^{comp} were co-incubated with human
359 PBMCs for 24 hours, followed by analysis of cytokine secretion in cell-free supernatants. As
360 compared with *B. longum* **35624**, the sEPS^{neg} strain was shown to induce higher levels of IL-
361 12p70, IFN- γ and IL-17 secretion, with comparable induction of IL-10 (Fig. 2A). The
362 sEPS^{comp} strain induced similar levels of cytokine secretion as *B. longum* **35624**, confirming
363 that enhanced pro-inflammatory cytokine secretion is specifically associated with the lack of
364 exopolysaccharide production. The addition of isolated exopolysaccharide to the co-cultures
365 significantly reduced IL-12p70 and IFN- γ secretion in response to the sEPS^{neg} strain, but did
366 not alter IL-17 or IL-10 responses to the sEPS^{neg} strain (Fig. 2B).

367 Similarly to PBMCs, human MDDCs were co-incubated with *B. longum* **35624** or
368 sEPS^{neg} strains, and cytokine secretion was measured after a 24 hour exposure. Secreted IL-
369 17, IL-6 and TNF- α levels, but not IL-10, were all shown to be significantly higher for the
370 sEPS^{neg}-stimulated MDDCs, compared to *B. longum* **35624** -stimulated MDDCs (Fig. 3A). In
371 contrast, no differences were found in the *B. longum* **35624** or sEPS^{neg} -induced expression of
372 the MDDC inhibitory molecules programmed death-ligand 1 (PD-L1) and PD-L2, which bind

373 to PD-1 on activated lymphocytes and play an important role in down-regulating the immune
374 system (Fig. 3B).

375 Activation of the transcription factor NF- κ B is critical for the induction of
376 inflammatory genes, including cytokines. Thus, we measured NF- κ B activation in the
377 monocyte cell line THP-1, containing a SEAP reporter for NF- κ B and AP-1 activation. The
378 sEPS^{neg} strain was shown to induce higher levels of NF- κ B/AP-1 activation, compared to *B.*
379 *longum* **35624**-stimulated THP-1 cells (Fig. 3C). To confirm this result, NF- κ B
380 phosphorylation was measured in MDDCs over time, following exposure to bacteria. Both *B.*
381 *longum* **35624** and sEPS^{neg} strains induced similar levels of NF- κ B phosphorylation at early
382 time points (Fig. 3D). However, sustained high levels of phosphorylated NF- κ B were
383 observed at later time points for the sEPS^{neg}-stimulated MDDCs, which were not observed for
384 *B. longum* **35624**-stimulated cells.

385 Taken together, these results suggest a role for this exopolysaccharide in preventing *in*
386 *vitro* inflammatory responses to *B. longum* **35624**.

387 **The sEPS^{neg} strain does not protect against colitis development.** Colitis was
388 induced in SCID mice by adoptively transferring CD4⁺CD25⁻CD45RB^{hi} lymphocytes. Mice
389 were administered *B. longum* **35624**, sEPS^{neg} or sEPS^{comp} daily by oral gavage. As previously
390 described, *B. longum* **35624** treatment prevented weight loss and disease symptoms in this
391 model (34). However, mice treated with the sEPS^{neg} strain exhibited significant weight loss
392 and severe disease symptoms, while restoration of EPS production in the sEPS^{comp} strain
393 promoted a similar response as to *B. longum* **35624** (Fig. 4A). Following euthanasia, the
394 colon:body weight ratio was significantly higher in animals administered the sEPS^{neg} strain,

395 while macroscopically the colons of these mice appeared severely inflamed with visible
396 necrotic regions, which was not observed when animals had been administered *B. longum*
397 **35624** (Fig. 4B). Within the mesenteric lymph nodes, there were significantly more IL-17⁺
398 lymphocytes in animals administered the sEPS^{neg}, with a trend towards increased numbers of
399 IFN- γ ⁺ lymphocytes, which was not statistically significant (Fig. 4C). No significant
400 difference in IL-10⁺ lymphocytes was observed. No differences in the gastrointestinal transit
401 of *B. longum* **35624** or the sEPS^{neg} derivative was observed (Supplementary Fig. S2).

402 The administration of the sEPS^{neg} strain to healthy immunocompetent animals did not result
403 in gastrointestinal inflammation, indicating that the sEPS^{neg} mutant did not induce colitis in
404 healthy animals. However, administration of sEPS^{neg} did provoke a trend in an increased
405 percentage of IL-17⁺ and IFN- γ ⁺ lymphocytes, associated with an increase in CCR9⁺ T cells,
406 within the lamina propria of healthy animals, although these differences did not reach
407 statistical significance (Supplementary Fig. S3). These data suggest that an inflamed micro-
408 environment, such as that present in the SCID model, is required for sEPS^{neg} to exert its T_H17-
409 enhancing effects.

410 **sEPS^{neg} exacerbates IL-17 responses within the lung.** In order to further assess the
411 ability of sEPS^{neg} to promote IL-17 responses *in vivo*, we utilized the ovalbumin (OVA)
412 sensitization and respiratory challenge model, as we and others previously evidenced potent
413 T_H17 responses within the lungs of challenged animals (35). Either the *B. longum* **35624** or its
414 isogenic derivative sEPS^{neg} were administered intra-nasally to examine the influence of these
415 strains on IL-17 responses within the lung. OVA sensitization and challenge resulted in an
416 increased percentage of IL-17⁺ lymphocytes within lung tissue, compared to control animals
417 (Fig. 5A). Exposure to the *B. longum* **35624** strain did not influence the percentage of IL-17⁺

418 lymphocytes within the lung, however, exposure to sEPS^{neg} significantly increased the
419 percentage of IL-17⁺ lymphocytes (Fig. 5A). Single cell suspensions were generated from the
420 lungs of all animals challenged as indicated above, and these lung cells were re-stimulated *ex*
421 *vivo* with OVA or LPS to assess IL-17 secretion. OVA sensitized and challenged animals
422 displayed increased *ex vivo* secretion of IL-17 to both OVA and LPS stimulation, compared to
423 non-sensitized animals, suggesting that innate TLR-4 responses to LPS and allergen-specific
424 lymphocyte responses to OVA are increased in the inflamed lungs of allergic animals (Fig.
425 5A). The *in vivo* exposure to *B. longum* **35624** did not alter the *ex vivo* secretion of IL-17 by
426 lung cells stimulated with either LPS or OVA. However, if animals had been exposed to
427 sEPS^{neg} *in vivo* previously, the isolated lung cells secreted significantly more IL-17 *ex vivo* in
428 response to both TLR-4 stimulation with LPS and allergen restimulation with OVA (Fig. 5A).
429 Thus, *ex vivo* secretion of IL-17 and the percentage of IL-17⁺ cells within lung tissue correlate
430 with the highest levels for both assay systems being observed for sEPS^{neg}-treated animals.

431 OVA sensitization and challenge resulted in an increased percentage of IFN- γ ⁺
432 lymphocytes within lung tissue, compared to control animals (Fig. 5A). Exposure to the *B.*
433 *longum* **35624** strain prevented the increase in the percentage of IFN- γ ⁺ lymphocytes within
434 the lung, which was not observed following exposure to the sEPS^{neg} strain (Fig. 5B). Re-
435 stimulation of lung single cell suspensions *ex vivo* with OVA or LPS did not result in
436 significant levels of IFN- γ being secreted and no statistically significant differences were
437 observed between the groups (Fig. 5B).

438 OVA sensitization and challenge resulted in an increased percentage of IL-10⁺
439 lymphocytes within lung tissue and exposure to *B. longum* **35624** or the sEPS^{neg} strains
440 further increased the percentage of IL-10⁺ lymphocytes within the lung (Fig. 5C). Re-

441 stimulation *ex vivo* was also associated with increased secretion of IL-10 following *in vivo*
442 exposure to *B. longum* **35624** or the sEPS^{neg} strains (Fig. 5C).

443 These findings suggest that the absence of the exopolysaccharide on *B. longum* **35624**
444 promotes T_H17 responses in the inflamed lung, similar to the effects described above for the
445 inflamed gut.

446

447 **DISCUSSION**

448 In order to avoid immune-mediated destruction of mucosal tissues, the host can activate
449 regulatory mechanisms that can block proinflammatory responses to commensal microbes
450 present on mucosal surfaces. Bifidobacteria comprise a significant proportion of the gut
451 microbiota and many strains are currently used as probiotics. However, the precise
452 mechanisms by which such bifidobacteria interact with host immune cells are not fully
453 understood. In this report we describe that the presence of a cell surface-associated
454 exopolysaccharide produced by *B. longum* **35624** modulates cytokine secretion and NF- κ B
455 activation *in vitro*, while in murine models exposure to a *B. longum* **35624** derivative unable
456 to synthesize exopolysaccharide promotes T_H17 responses both within the gut and the lung.

457 Bifidobacterial cell surface-associated exopolysaccharides have previously been
458 proposed to (i) mediate some of their health-promoting benefits, (ii) contribute to their
459 tolerance of the harsh conditions within the gut, and (iii) to influence composition of the gut
460 microbiome through their use as a fermentable substrate by other microbes (36-39). In
461 general, bacterial exopolysaccharide consists of repeating mono- or oligosaccharide subunits
462 connected by varying glycosidic linkages, which are structurally very diverse, and which may

463 contribute to strain-specific traits due to the expected structural and therefore functional
464 diversity of such molecules. Of note, pathogen-associated exopolysaccharides have long been
465 known to be critical in host–microbe interactions, where they facilitate adherence and
466 colonization within the human host, with additional immunomodulatory effects (40, 41).
467 Exopolysaccharides can also mediate the beneficial immune effects associated with certain
468 commensal microbes. As already mentioned, a strong modulator of intestinal immune
469 responses is PSA from *B. fragilis*, which is well described to influence lymphocyte
470 polarization and PSA suppresses IL-17 production by intestinal immune cells (42-44). In line
471 with data presented in this manuscript, exopolysaccharide gene knockout mutants of
472 *Lactobacillus casei* Shirota induced significantly more pro-inflammatory cytokine secretion
473 from a mouse macrophage cell line, compared to wild-type cells (45). In addition, the
474 cytokine response of PBMCs to two isogenic strains of *B. animalis* subsp. *lactis* that differ
475 only in their exopolysaccharide-producing phenotype suggest that the mucoid strain could
476 have higher anti-inflammatory activity (31). The data presented in this manuscript are in
477 agreement with these previous reports and further supports the concept that
478 exopolysaccharides from bifidobacteria may elicit immune-modulatory activities.

479 Interestingly, the induction of PD-L1 and PD-L2 on dendritic cells was similar for the
480 wild type *B. longum* **35624** strain and its isogenic derivative sEPS^{neg}. Similarly, the induction
481 of IL-10 was not negatively impacted by the loss of exopolysaccharide from the bacterium.
482 This suggests that not all immune-regulatory effects induced by *B. longum* **35624** are
483 mediated solely by exopolysaccharide. The bifidobacterial cell wall is a complex arrangement
484 of macromolecules, consisting of a thick peptidoglycan layer that surrounds the cytoplasmic
485 membrane, which is decorated with other glycopolymers, such as (lipo)teichoic acids,
486 polysaccharides and proteins, all of which may influence the immune response (46, 47) A few
22

487 examples include the cell wall-associated proteins p40 and p75 from *L. casei* ssp. *rhamnosus*
488 GG, the S-layer protein from *L. acidophilus*, or the STp peptide from *L. plantarum* (48-50) .

489 T_H17 cells are a subset of CD4⁺ T helper cells that mediate protective immunity to
490 extracellular bacterial and fungal pathogens, predominantly at epithelial surfaces (51).
491 Polarization of naïve T cells into T_H17 cells occurs following T-cell antigen receptor
492 recognition of an MHC class II-bound peptide in the presence of cytokines including TGF- β 1,
493 IL-6 or IL-1 β (52, 53). While T_H17 cells are required for protective immunity, these cells
494 massively infiltrate the inflamed intestine of inflammatory bowel disease patients, where they
495 produce IL-17 and other cytokines, triggering and amplifying the inflammatory process (54).
496 Our data suggests that the *B. longum* **35624** strain-associated exopolysaccharide prevents the
497 induction of a T_H17 response to this bacterium. Multiple mechanisms may be involved in this
498 process. For example the exaggerated induction of cytokines, including IL-6, from dendritic
499 cells may support T_H17 lymphocyte polarization and development. Support for this
500 hypothesis can be seen when we restimulate OVA-specific T cells with OVA and we observe
501 increased secretion of IL-17 when the lungs were previously exposed to sEPS^{neg}. These OVA-
502 specific T cells are not reacting to bifidobacteria-associated antigens, but more IL-17 is
503 secreted upon OVA challenge suggesting that it is the cytokine microenvironment, provided
504 by innate cells such as dendritic cells, that is supporting excessive T_H17 development. The
505 observation that addition of purified exopolysaccharide to sEPS^{neg}-stimulated PBMCs
506 suppresses the exaggerated IL-12p70 and IFN- γ secretion, but not IL-17 secretion, also
507 suggests that multiple mechanisms may be involved. Future studies will determine if it is the
508 exopolysaccharide itself that can directly inhibit T_H17 responses by binding to host receptors,

509 or if the exopolysaccharide is simply masking T_H17-promoting molecules on the surface of
510 this bacterium.

511 In conclusion, we have identified a novel immunoregulatory activity associated with
512 the presence of a exopolysaccharide in the human commensal *B. longum* 35624 strain. Our
513 findings suggest that this exopolysaccharide is required to prevent a potent tissue-damaging
514 T_H17 response to a commensal bacterium. Accordingly, our data on the *B. longum* 35624-
515 associated exopolysaccharide corroborates, and expands, the published concept that
516 exopolysaccharides produced by certain lactic acid bacteria and bifidobacteria may elicit
517 immune-modulatory activities (55), which are important for appropriate host-microbe
518 communication.

519

520 **Funding information.** These studies were directly supported by a European Union Marie
521 Curie training network, entitled “TEAM-EPIC”. In addition, the authors are supported by
522 Swiss National Foundation grants (project numbers CRSII3_154488 and 310030_144219),
523 Christine Kühne Center for Allergy Research and Education, and by Science Foundation
524 Ireland (SFI) (Grant No. SFI/12/RC/2273). Mary O'Connell Motherway is a recipient of a
525 HRB postdoctoral fellowship (Grant No. PDTM/20011/9). Elisa Schiavi was supported by an
526 EAACI Research Fellowship Award 2012.

527 The funders had no role in study design, data collection and interpretation, or the decision to
528 submit the work for publication.

529

530 **Acknowledgments.** 35624 is a trademark of Alimentary Health Ltd, Cork, Ireland. We thank
531 Patrycja Konieczna for her technical assistance.

532

533 REFERENCES

- 534 1. **Donaldson GP, Lee SM, Mazmanian SK.** 2016. Gut biogeography of the bacterial microbiota.
535 Nat Rev Microbiol **14**:20-32.
- 536 2. **Marchesi JR, Adams DH, Fava F, Hermes GDA, Hirschfield GM, Hold G, Quraishi MN, Kinross**
537 **J, Smidt H, Tuohy KM, Thomas LV, Zoetendal EG, Hart A.** 2016. The gut microbiota and host
538 health: a new clinical frontier. Gut **65**:330-339.
- 539 3. **Frei R, Lauener RP, Cramer R, O'Mahony L.** 2012. Microbiota and dietary interactions - an
540 update to the hygiene hypothesis? Allergy **67**:451-461.
- 541 4. **Trompette A, Gollwitzer ES, Yadava K, Sichelstiel AK, Sprenger N, Ngom-Bru C, Blanchard C,**
542 **Junt T, Nicod LP, Harris NL, Marsland BJ.** 2014. Gut microbiota metabolism of dietary fiber
543 influences allergic airway disease and hematopoiesis. Nat Med **20**:159-166.
- 544 5. **Frei R, Akdis M, O'Mahony L.** 2015. Prebiotics, probiotics, synbiotics, and the immune
545 system: experimental data and clinical evidence. Curr Opin Gastroenterol **31**:153-158.
- 546 6. **Tomkovich S, Jobin C.** 2016. Microbiota and host immune responses: a love-hate
547 relationship. Immunology **147**:1-10.
- 548 7. **Konieczna P, Akdis CA, Quigley EMM, Shanahan F, O'Mahony L.** 2012. Portrait of an
549 immunoregulatory Bifidobacterium. Gut Microbes **3**:261-266.
- 550 8. **O'Mahony C, Scully P, O'Mahony D, Murphy S, O'Brien F, Lyons A, Sherlock G, MacSharry J,**
551 **Kiely B, Shanahan F, O'Mahony L.** 2008. Commensal-Induced Regulatory T Cells Mediate
552 Protection against Pathogen-Stimulated NF- κ B Activation. PLoS Pathogens **4**:e1000112.
- 553 9. **Lyons A, O'Mahony D, O'Brien F, MacSharry J, Sheil B, Ceddia M, Russell WM, Forsythe P,**
554 **Bienenstock J, Kiely B, Shanahan F, O'Mahony L.** 2010. Bacterial strain-specific induction of
555 Foxp3 + T regulatory cells is protective in murine allergy models. Clin Exp Allergy **40**:811-9.
- 556 10. **McCarthy J, O'Mahony L, O'Callaghan L, Sheil B, Vaughan EE, Fitzsimons N, Fitzgibbon J,**
557 **O'Sullivan GC, Kiely B, Collins JK, Shanahan F.** 2003. Double blind, placebo controlled trial of
558 two probiotic strains in interleukin 10 knockout mice and mechanistic link with cytokine
559 balance. Gut **52**:975-980.
- 560 11. **Scully P, MacSharry J, O'Mahony D, Lyons A, O'Brien F, Murphy S, Shanahan F, O'Mahony L.**
561 **2013. Bifidobacterium infantis** suppression of Peyer's patch MIP-1 α and MIP-1 β secretion
562 during *Salmonella* infection correlates with increased local CD4+CD25+ T cell numbers. Cell
563 Immunol **281**:134-140.
- 564 12. **Symonds EL, O'Mahony C, Laphorne S, O'Mahony D, Sharry JM, O'Mahony L, Shanahan F.**
565 **2012. Bifidobacterium Infantis 35624** Protects Against Salmonella-Induced Reductions in
566 Digestive Enzyme Activity in Mice by Attenuation of the Host Inflammatory Response. Clin
567 Transl Gastroenterol **3**:e15.
- 568 13. **Konieczna P, Groeger D, Ziegler M, Frei R, Ferstl R, Shanahan F, Quigley EMM, Kiely B, Akdis**
569 **CA, O'Mahony L.** 2012. *Bifidobacterium infantis* 35624 administration induces Foxp3 T
570 regulatory cells in human peripheral blood: potential role for myeloid and plasmacytoid
571 dendritic cells. Gut **61**:354-366.

25

- 572 14. **Groeger D, O'Mahony L, Murphy EF, Bourke JF, Dinan TG, Kiely B, Shanahan F, Quigley**
573 **EMM.** 2013. *Bifidobacterium infantis* 35624 modulates host inflammatory processes beyond
574 the gut. *Gut Microbes* **4**:325-339.
- 575 15. **Konieczna P, Ferstl R, Ziegler M, Frei R, Nehrbass D, Lauener RP, Akdis CA, O'Mahony L.**
576 2013. Immunomodulation by *Bifidobacterium infantis* 35624 in the Murine Lamina Propria
577 Requires Retinoic Acid-Dependent and Independent Mechanisms. *PLoS One* **8**:e62617.
- 578 16. **Sibartie S, O'Hara AM, Ryan J, Fanning A, O'Mahony J, O'Neill S, Sheil B, O'Mahony L,**
579 **Shanahan F.** 2009. Modulation of pathogen-induced CCL20 secretion from HT-29 human
580 intestinal epithelial cells by commensal bacteria. *BMC Immunol* **10**:54.
- 581 17. **O'Mahony L, O'Callaghan L, McCarthy J, Shilling D, Scully P, Sibartie S, Kavanagh E, Kirwan**
582 **WO, Redmond HP, Collins JK, Shanahan F.** 2006. Differential cytokine response from
583 dendritic cells to commensal and pathogenic bacteria in different lymphoid compartments in
584 humans. *Am J Physiol Gastrointest Liver Physiol* **290**:839-845.
- 585 18. **Round JL, Mazmanian SK.** 2010. Inducible Foxp3+ regulatory T-cell development by a
586 commensal bacterium of the intestinal microbiota. *Proc Natl Acad Sci U S A* **107**:12204-
587 12209.
- 588 19. **Dasgupta S, Erturk-Hasdemir D, Ochoa-Reparaz J, Reinecker HC, Kasper DL.** 2014.
589 Plasmacytoid dendritic cells mediate anti-inflammatory responses to a gut commensal
590 molecule via both innate and adaptive mechanisms. *Cell Host Microbe* **15**:413-423.
- 591 20. **Jones SE, Paynich ML, Kearns DB, Knight KL.** 2014. Protection from intestinal inflammation
592 by bacterial exopolysaccharides. *J Immunol* **192**:4813-4820.
- 593 21. **Fanning S, Hall LJ, Cronin M, Zomer A, MacSharry J, Goulding D, Motherway MO, Shanahan**
594 **F, Nally K, Dougan G, van Sinderen D.** 2012. Bifidobacterial surface-exopolysaccharide
595 facilitates commensal-host interaction through immune modulation and pathogen
596 protection. *Proc Natl Acad Sci U S A* **109**:2108-2113.
- 597 22. **Rossi O, Khan MT, Schwarzer M, Hudcovic T, Srutkova D, Duncan SH, Stolte EH, Kozakova H,**
598 **Flint HJ, Samsom JN, Harmsen HJ, Wells JM.** 2015. *Faecalibacterium prausnitzii* Strain HTF-F
599 and Its Extracellular Polymeric Matrix Attenuate Clinical Parameters in DSS-Induced Colitis.
600 *PLoS One* **10**:e0123013.
- 601 23. **Altmann F AF, Kosma P, O'Callaghan A, Leahy S, Bottacini F, Molloy E, Plattner S, Schiavi E,**
602 **Gleinser M, Groeger D, Grant R, Rodriguez Perez N, Healy S, Svehla E, Windwarder M,**
603 **Hofinger A, O'Connell Motherway M, Akdis CA, Xu J, Roper J, van Sinderen D, O'Mahony L.**
604 2016. Genome Analysis and Characterisation of the Exopolysaccharide Produced by
605 *Bifidobacterium longum* subsp. *longum* 35624. *PLoS ONE* **11**: e0162983.
- 606 24. **O'Riordan, Fitzgerald.** 1998. Evaluation of bifidobacteria for the production of antimicrobial
607 compounds and assessment of performance in cottage cheese at refrigeration temperature. *J*
608 *Appl Microbiol* **85**:103-114.
- 609 25. **Maze A, O'Connell-Motherway M, Fitzgerald GF, Deutscher J, van Sinderen D.** 2006.
610 Identification and Characterization of a Fructose Phosphotransferase System in
611 *Bifidobacterium breve* UCC2003. *Appl Environ Microbiol* **73**:545-553.
- 612 26. **Law J, Buist G, Haandrikman A, Kok J, Venema G, Leenhouts K.** 1995. A system to generate
613 chromosomal mutations in *Lactococcus lactis* which allows fast analysis of targeted genes. *J*
614 *Bacteriol* **177**:7011-7018.
- 615 27. **Alvarez-Martín P, O'Connell-Motherway M, van Sinderen D, Mayo B.** 2007. Functional
616 analysis of the pBC1 replicon from *Bifidobacterium catenulatum* L48. *Appl Microbiol*
617 *Biotechnol* **76**:1395-1402.
- 618 28. **Masuko T, Minami A, Iwasaki N, Majima T, Nishimura SI, Lee YC.** 2005. Carbohydrate
619 analysis by a phenol-sulphuric acid method in microplate format. *Analytical Biochemistry*
620 **339**:69-72.
- 26

- 621 29. **Arnold IC, Hutchings C, Kondova I, Hey A, Powrie F, Beverley P, Tchilian E.** 2015.
622 *Helicobacter hepaticus* infection in BALB/c mice abolishes subunit-vaccine-induced
623 protection against *M. tuberculosis*. *Vaccine* **33**:1808-1814.
- 624 30. **O'Connell Motherway M, O'Driscoll J, Fitzgerald GF, Van Sinderen D.** 2009. Overcoming the
625 restriction barrier to plasmid transformation and targeted mutagenesis in *Bifidobacterium*
626 *breve* UCC2003. *Microb Biotechnol* **2**:321-332.
- 627 31. **Hidalgo-Cantabrana C, Sanchez B, Alvarez-Martin P, Lopez P, Martinez-Alvarez N, Delley M,**
628 **Marti M, Varela E, Suarez A, Antolin M, Guarner F, Berger B, Ruas-Madiedo P, Margolles A.**
629 2015. A single mutation in the gene responsible for the mucoid phenotype of
630 *Bifidobacterium animalis* subsp. *lactis* confers surface and functional characteristics. *Appl*
631 *Environ Microbiol* **81**:7960-7968.
- 632 32. **Egan M, O'Connell Motherway M, Ventura M, van Sinderen D.** 2014. Metabolism of sialic
633 acid by *Bifidobacterium breve* UCC2003. *Appl Environ Microbiol* **80**:4414-4426.
- 634 33. **O'Connell Motherway M, Kinsella M, Fitzgerald GF, van Sinderen D.** 2013. Transcriptional
635 and functional characterization of genetic elements involved in galacto-oligosaccharide
636 utilization by *Bifidobacterium breve* UCC2003. *Microb Biotechnol* **6**:67-79.
- 637 34. **van der Kleij H, O'Mahony C, Shanahan F, O'Mahony L, Bienenstock J.** 2008. Protective
638 effects of *Lactobacillus reuteri* and *Bifidobacterium infantis* in murine models for colitis do
639 not involve the vagus nerve. *Am J Physiol Regul Integr Comp Physiol* **295**:R1131-R1137.
- 640 35. **Lu S, Li H, Gao R, Gao X, Xu F, Wang Q, Lu G, Xia D, Zhou J.** 2016. IL-17A, But Not IL-17F, Is
641 Indispensable for Airway Vascular Remodeling Induced by Exaggerated Th17 Cell Responses
642 in Prolonged Ovalbumin-Challenged Mice. *J Mol Med (Berl)* **194**:3557-3566.
- 643 36. **Fanning S, Hall LJ, Cronin M, Zomer A, MacSharry J, Goulding D, O'Connell Motherway M,**
644 **Shanahan F, Nally K, Dougan G, van Sinderen D.** 2012. Bifidobacterial surface-
645 exopolysaccharide facilitates commensal-host interaction through immune modulation and
646 pathogen protection. *Proc Natl Acad Sci U S A* **109**:2108-2113.
- 647 37. **Salazar N, Ruas-Madiedo P, Kolida S, Collins M, Rastall R, Gibson G, de los Reyes-Gavilán**
648 **CG.** 2009. Exopolysaccharides produced by *Bifidobacterium longum* IPLA E44 and
649 *Bifidobacterium animalis* subsp. *lactis* IPLA R1 modify the composition and metabolic activity
650 of human faecal microbiota in pH-controlled batch cultures. *Int J Food Microbiol* **135**:260-
651 267.
- 652 38. **Alp G, Aslim B.** 2010. Relationship between the resistance to bile salts and low pH with
653 exopolysaccharide (EPS) production of *Bifidobacterium* spp. isolated from infants feces and
654 breast milk. *Anaerobe* **16**:101-105.
- 655 39. **Salazar N, Gueimonde M, de los Reyes-Gavilán CG, Ruas-Madiedo P.** 2016.
656 Exopolysaccharides Produced by Lactic Acid Bacteria and Bifidobacteria as Fermentable
657 Substrates by the Intestinal Microbiota. *Crit Rev Food Sci Nutr* **56**:1440-1453.
- 658 40. **Conover MS, Sloan GP, Love CF, Sukumar N, Deora R.** 2010. The Bps polysaccharide of
659 *Bordetella pertussis* promotes colonization and biofilm formation in the nose by functioning
660 as an adhesin. *Mol Microbiol* **77**:1439-1455.
- 661 41. **Xu CL, Wang YZ, Jin ML, Yang XQ.** 2009. Preparation, characterization and
662 immunomodulatory activity of selenium-enriched exopolysaccharide produced by bacterium
663 *Enterobacter cloacae* Z0206. *Bioresour Technol* **100**:2095-2097.
- 664 42. **Round JL, Lee SM, Li J, Tran G, Jabri B, Chatila TA, Mazmanian SK.** 2011. The Toll-like
665 receptor 2 pathway establishes colonization by a commensal of the human microbiota.
666 *Science* **332**:974-977.
- 667 43. **Mazmanian SK, Liu CH, Tzianabos AO, Kasper DL.** 2005. An immunomodulatory molecule of
668 symbiotic bacteria directs maturation of the host immune system. *Cell* **122**:107-118.

- 669 44. **Mazmanian SK, Round JL, Kasper DL.** 2008. A microbial symbiosis factor prevents intestinal
670 inflammatory disease. *Nature* **453**:620-625.
- 671 45. **Yasuda E, Serata M, Sako T.** 2008. Suppressive effect on activation of macrophages by
672 *Lactobacillus casei* strain Shirota genes determining the synthesis of cell wall-associated
673 polysaccharides. *Appl Environ Microbiol* **74**:4746-4755.
- 674 46. **Chapot-Chartier M-P, Kulakauskas S.** 2014. Cell wall structure and function in lactic acid
675 bacteria. *Microb Cell Fact* **13**:S9.
- 676 47. **Ruiz L, Hevia A, Bernardo D, Margolles A, Sánchez B.** 2014. Extracellular molecular effectors
677 mediating probiotic attributes. *FEMS Microbiol Lett* **359**:1-11.
- 678 48. **Konstantinov SR, Smidt H, de Vos WM, Bruijns SCM, Singh SK, Valence F, Molle D, Lortal S,**
679 **Altermann E, Klaenhammer TR, van Kooyk Y.** 2008. S layer protein A of *Lactobacillus*
680 *acidophilus* NCFM regulates immature dendritic cell and T cell functions. *Proc Natl Acad Sci U*
681 *S A* **105**:19474-19479.
- 682 49. **Al-Hassi HO, Mann ER, Sanchez B, English NR, Peake STC, Landy J, Man R, Urdaci M, Hart**
683 **AL, Fernandez-Salazar L, Lee GH, Garrote JA, Arranz E, Margolles A, Stagg AJ, Knight SC,**
684 **Bernardo D.** 2013. Altered human gut dendritic cell properties in ulcerative colitis are
685 reversed by *Lactobacillus plantarum* extracellular encrypted peptide STp. *Mol Nutr Food Res*
686 **58**:1132-1143.
- 687 50. **Yan F, Cao H, Cover TL, Washington MK, Shi Y, Liu L, Chaturvedi R, Peek RM, Wilson KT,**
688 **Polk DB.** 2011. Colon-specific delivery of a probiotic-derived soluble protein ameliorates
689 intestinal inflammation in mice through an EGFR-dependent mechanism. *J Clin Invest*
690 **121**:2242-2253.
- 691 51. **Korn T, Bettelli E, Oukka M, Kuchroo VK.** 2009. IL-17 and Th17 Cells. *Annu Rev Immunol*
692 **27**:485-517.
- 693 52. **Veldhoen M, Hocking RJ, Atkins CJ, Locksley RM, Stockinger B.** 2006. TGF β in the Context of
694 an Inflammatory Cytokine Milieu Supports De Novo Differentiation of IL-17-Producing T Cells.
695 *Immunity* **24**:179-189.
- 696 53. **Akdis M, Burgler S, Cramer R, Eiwegger T, Fujita H, Gomez E, Klunker S, Meyer N,**
697 **O'Mahony L, Palomares O, Rhyner C, Ouaked N, Schaffartzik A, Van De Veen W, Zeller S,**
698 **Zimmermann M, Akdis CA.** 2011. Interleukins, from 1 to 37, and interferon- γ : receptors,
699 functions, and roles in diseases. *J Allergy Clin Immunol* **127**:701-721.
- 700 54. **Gálvez J.** 2014. Role of Th17 Cells in the Pathogenesis of Human IBD. *ISRN Inflammation*
701 **2014**:1-14.
- 702 55. **Hidalgo-Cantabrana C, Lopez P, Gueimonde M, de Los Reyes-Gavilan CG, Suarez A,**
703 **Margolles A, Ruas-Madiedo P.** 2012. Immune Modulation Capability of Exopolysaccharides
704 Synthesised by Lactic Acid Bacteria and Bifidobacteria. *Probiotics Antimicrob Proteins* **4**:227-
705 237.
- 706 56. **Margolles A, Florez AB, Moreno JA, van Sinderen D, de los Reyes-Gavilan CG.** 2006. Two
707 membrane proteins from *Bifidobacterium breve* UCC2003 constitute an ABC-type multidrug
708 transporter. *Microbiology* **152**:3497-3505.
- 709
710

711

712 **FIGURE LEGENDS**

713 **Figure 1.** *B. longum* **35624** electron microscopy

714 Representative scanning electron microscopy (SEM) images for the *B. longum* **35624** parent
715 strain (A, upper panel) and its isogenic derivatives, sEPS^{neg} mutant (B, middle panel) and
716 sEPS^{comp} mutant (C, bottom panel) are illustrated. Arrows indicate the ‘stringy’ layer of
717 extracellular polysaccharide visible on the *B. longum* **35624** parent strain and sEPS^{comp} strain.
718 Scale bars are indicated at the bottom right of each panel.

719

720 **Figure 2.** PBMC cytokine response to bacterial strains

721 (A) PBMCs from 6 healthy donors were stimulated with *B. longum* **35624** or its isogenic
722 derivatives sEPS^{neg} or sEPS^{comp} (50 bacteria:1 PBMC) for 24 hours and cytokine secretion
723 into the culture supernatant was quantified. Data are presented as box-and-whisker plots with
724 the median value and max/min values illustrated. Statistical significance was determined
725 using the Kruskal–Wallis test and Dunn’s multiple comparison test (*p<0.05). (B) Effect of
726 adding isolated exopolysaccharide on sEPS^{neg} strain-induced PBMC secretion of IL-12p70,
727 IFN-gamma, IL-17 and IL-10. Each line connects the data from the same donor. The Mann–
728 Whitney U test was used for the statistical analysis (*p<0.05 versus the sEPS^{neg} strain alone).

729

730 **Figure 3.** MDDC response to bacterial strains

731 MDDCs were generated from 4 healthy donors and were stimulated with *B. longum* **35624** or
732 its isogenic derivative sEPS^{neg} (50 bacteria:1 MDDC) for 24 hours. Cytokine secretion into

29

733 the culture supernatant (A) and cell surface expression of the inhibitory molecules PD-L1 or
734 PD-L2 (B) were quantified. Data are presented as box-and-whisker plots with the median
735 value and max/min values illustrated. The Mann–Whitney U test was used for the statistical
736 analysis (* $p < 0.05$ *B. longum* **35624** versus the sEPS^{neg} strain). (C) THP-1 NF- κ B activation
737 following exposure to increasing concentrations of *B. longum* **35624** or its isogenic derivative
738 sEPS^{neg} (n=4 experimental replicates). (D) Activation of NF- κ B in MDDCs exposed to *B.*
739 *longum* **35624** or its isogenic derivative sEPS^{neg} (n=3, 50 bacteria:1 MDDC) . Statistical
740 significance was determined using two-way ANOVA (* $p < 0.05$ *B. longum* **35624** versus the
741 sEPS^{neg} strain).

742

743 **Figure 4.** sEPS^{neg} is not protective in a T cell transfer colitis model

744 Following receipt of CD4⁺CD25⁻CD45RB^{hi} T cells, C.B-17 SCID mice were orally
745 administered *B. longum* **35624** (n=8), sEPS^{comp} (n=8) or sEPS^{neg} (n=8) strains. (A) Weight
746 loss and disease activity were monitored over time. Statistical significance was determined
747 using two-way ANOVA (* $p < 0.05$). (B) Following euthanasia, the colon:body weight ratio
748 was determined. A representative picture of colons from *B. longum* **35624** or sEPS^{neg}-treated
749 animals is provided. (C) The percentage of IL-17⁺, IFN- γ ⁺ and IL-10⁺ lymphocytes from
750 mesenteric lymph nodes are illustrated (n=8 per group). Data are presented as box-and-
751 whisker plots with the median value and max/min values illustrated. Statistical significance
752 was determined using the Kruskal–Wallis test and Dunn’s multiple comparison test (* $p < 0.05$
753 sEPS^{neg} strain versus the other strains).

754

755 **Figure 5.** sEPS^{neg} promotes T_H17 responses in the lung

756 Non-sensitized animals received an OVA aerosol challenge and were intranasally

757 administered PBS (Control, n=8). Sensitized animals received an OVA aerosol challenge and

758 were intranasally administered PBS (OVA, n=8), or intranasally administered *B. longum*

759 **35624** (OVA & 35624, n=8), or intranasally administered sEPS^{neg} (OVA & sEPS^{neg}, n=8).

760 (A) The percentage of IL-17⁺ CD3⁺CD4⁺ T lymphocytes, isolated from lung tissue, and

761 secretion of IL-17 from isolated lung cells re-stimulated *ex vivo* with OVA or LPS. Similarly,

762 IFN- γ ⁺ and IL-10⁺ CD3⁺CD4⁺ T lymphocytes and *ex vivo* IFN- γ and IL-10 secretion were

763 quantified using identical methods, (B) and (C) respectively. Data are presented as box-and-

764 whisker plots with the median value and max/min values illustrated. Statistical significance

765 was determined using the Kruskal–Wallis test and Dunn’s multiple comparison test (*p<0.05

766 compared to the OVA group).

767 **Table 1.** Bacterial strains and plasmids used in this study.

| <i>Strain or plasmid</i> | <i>Relevant characteristics</i> | <i>Reference or source</i> |
|---|--|--|
| Strains | | |
| <i>E. coli</i> EC101 | Cloning host, repA ⁻ , Km ^r | Law <i>et al.</i> , 1995 (26) |
| <i>E. coli</i> XL1blue | Cloning host, , Tet ^r | Stratagene |
| <i>E. coli</i> EC101 pNZ-M.1185 | <i>E. coli</i> EC101 harbouring pNZ-M.1185 | This study |
| <i>B. longum</i> 35624 | Parent strain | Alimentary Health |
| sEPS ^{neg} | <i>B. longum</i> 35624 harbouring insertion mutation in priming glycosyl transferase encoding gene, <i>pgt</i> ₆₂₄ | This study |
| sEPS ^{comp} | sEPS ^{neg} harbouring pBC1.2_ <i>pgt</i> ₆₂₄ + <i>BI0343</i> | This study |
| Plasmids | | |
| pNZEm | Gene expression vector, Em ^r | Margolles <i>et al.</i> , 2006 (56) |
| pORI19 | Em ^r , repA ⁻ , ori ⁺ , cloning vector | Law <i>et al.</i> , 1995 (25) |
| pORI19 <i>tet(w)_pgt</i> | pORI19 harbouring internal fragment of <i>BI0342</i> (<i>pgt</i>) and <i>tetW</i> gene | This study |
| pBC1.2 | <i>E. coli</i> –Bifidobacterial shuttle vector | Álvarez-Martín <i>et al.</i> , 2007 (27) |
| pBC1.2_ <i>pgt</i> ₆₂₄ + <i>BI0343</i> | pBC1.2 harbouring the cotranscribed genes <i>pgt</i> ₆₂₄ + <i>BI0343</i> under the control of their native promoter | This study |
| pNZ-M.1185 | <i>BI1185</i> (<i>M.1185</i> , isoschizomer of M.EcoRII) cloned with its own promoter in pNZEM | This study |

768

769

770 **Table 2.** Oligonucleotide primers used in this study are described.

| <i>Purpose</i> | <i>Primer</i> | <i>Sequence^a</i> |
|--|-----------------|--|
| Cloning of M.1185 in pNZEm | BI1185F_PstI | GACTGCAGGCCCACTAGGTAACCAAACG |
| | BI1185R_SpeI | GCGCACTAGTCTAGAGCAAAGCCAGTATAG |
| Cloning of internal 583 bp fragment of <i>pgt</i> in pOR119 | BI0342F_HindIII | GATAAGCTT GCGTCGGCAACTCAACTACC |
| | BI0342R_XbaI | GATTCTAGAC GC TCGGCTTCACTACCATC |
| Cloning of <i>pgt</i> ₆₂₄ +BI0343 in pBC1.2 | BI0342FSalI | GACGTCGAC ACTCCACTCTCGCTGATCG |
| | BI0343EcoRI | GGCGAATTCT AATCAACCAAGGGGGTCTG |

771 ^a Restriction sites incorporated into oligonucleotide primer sequences are indicated in bold

Figure 1

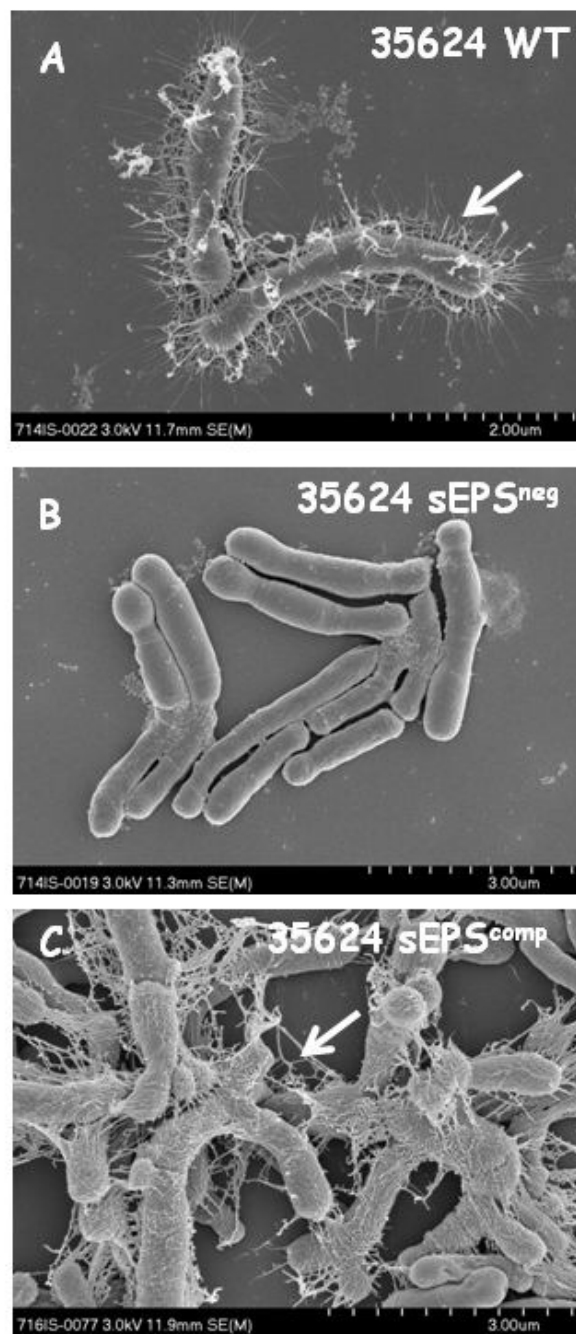
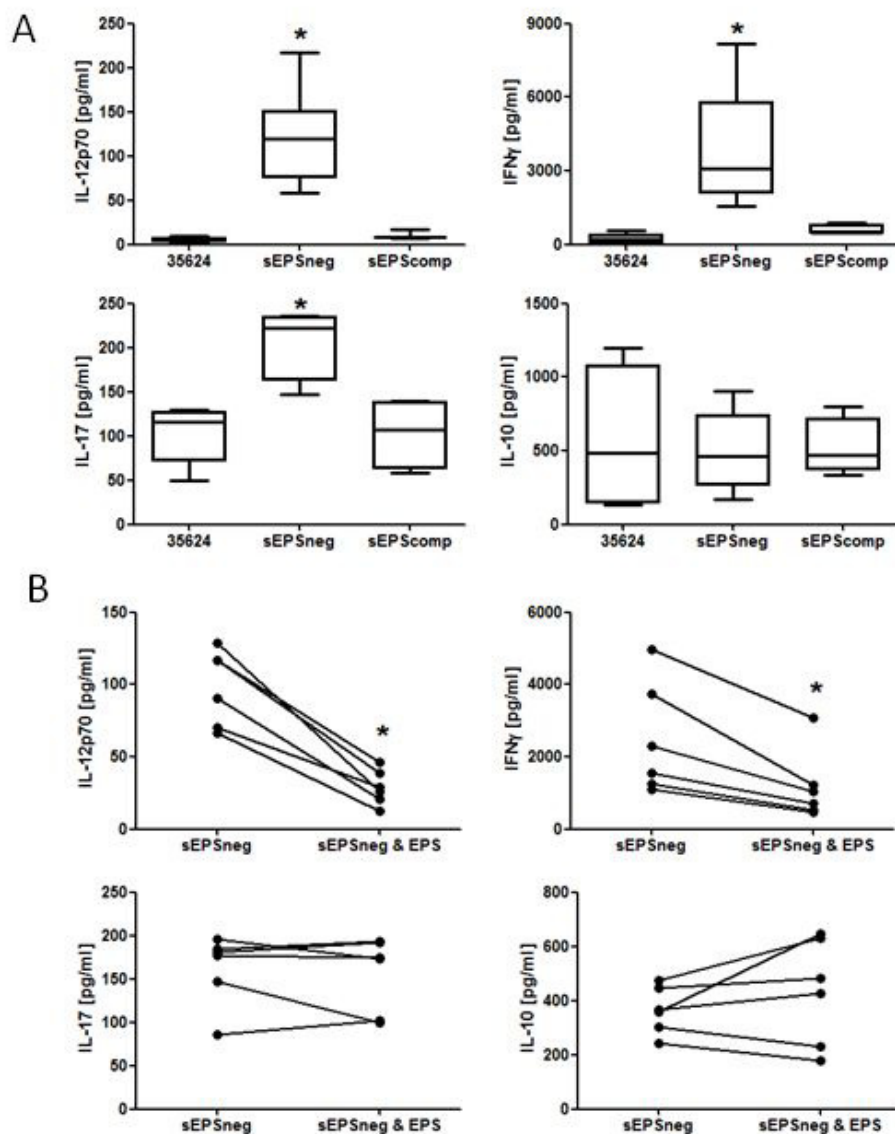


Figure 1. *B. longum* 35624 electron microscopy

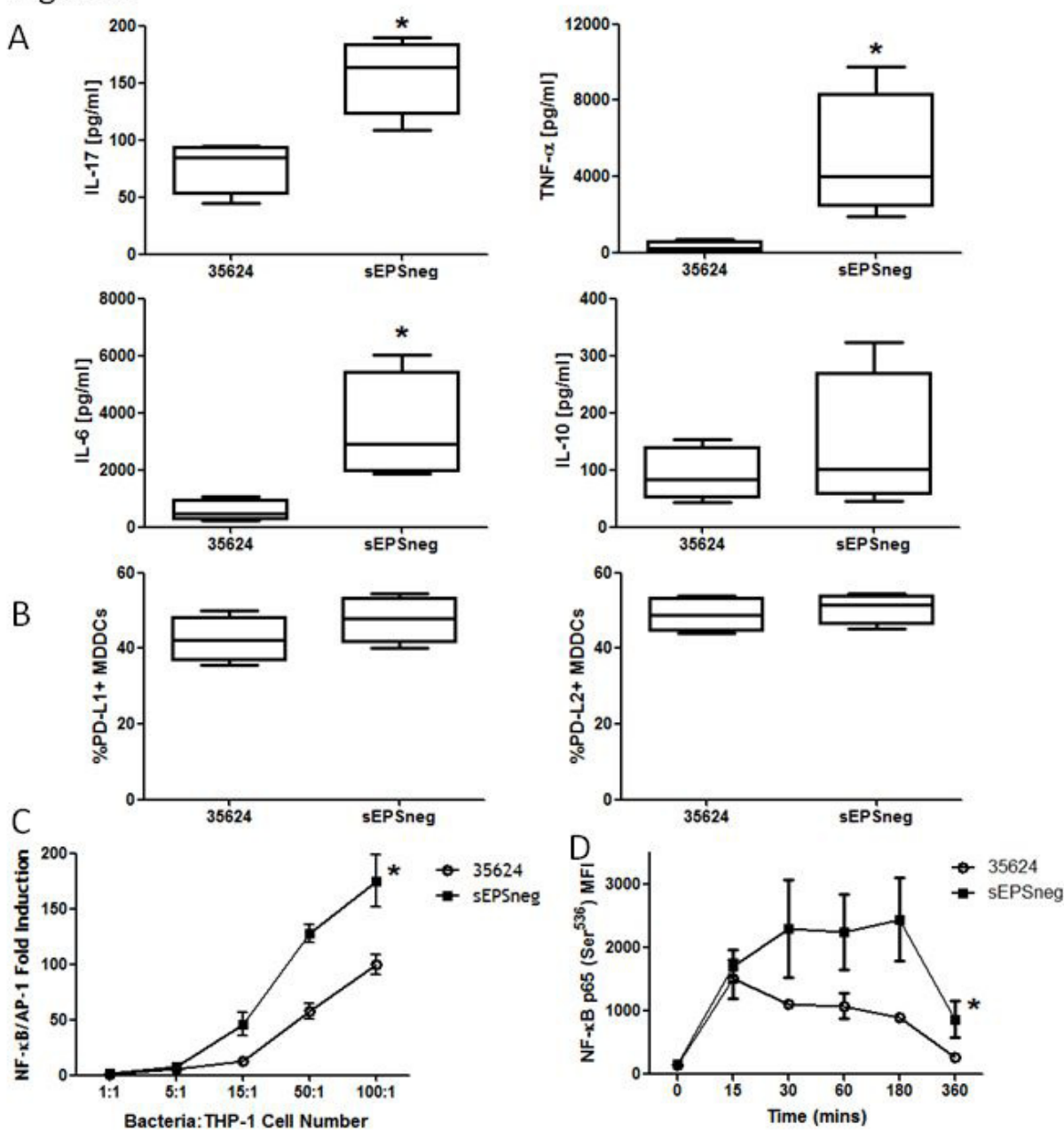
Representative scanning electron microscopy (SEM) images for the *B. longum* 35624 parent strain (A, upper panel) and its isogenic derivatives, sEPS^{neg} mutant (B, middle panel) and sEPS^{comp} mutant (C, bottom panel) are illustrated. Arrows indicate the 'stringy' layer of extracellular polysaccharide visible on the *B. longum* 35624 parent strain and sEPS^{comp} strain. Scale bars are indicated at the bottom right of each panel.

Figure 2

**Figure 2.** PBMC cytokine response to bacterial strains

(A) PBMCs from 6 healthy donors were stimulated with *B. longum* 35624 or its isogenic derivatives sEPS^{neg} or sEPS^{comp} (50 bacteria:1 PBMC) for 24 hours and cytokine secretion into the culture supernatant was quantified. Data are presented as box-and-whisker plots with the median value and max/min values illustrated. Statistical significance was determined using the Kruskal–Wallis test and Dunn’s multiple comparison test (* $p < 0.05$). (B) Effect of adding isolated exopolysaccharide on sEPS^{neg} strain-induced PBMC secretion of IL-12p70, IFN-gamma, IL-17 and IL-10. Each line connects the data from the same donor. The Mann–Whitney U test was used for the statistical analysis (* $p < 0.05$ versus the sEPS^{neg} strain alone).

Figure 3

**Figure 3.** MDDC response to bacterial strains

MDDCs were generated from 4 healthy donors and were stimulated with *B. longum* 35624 or its isogenic derivative sEPS^{neg} (50 bacteria: 1 MDDC) for 24 hours. Cytokine secretion into the culture supernatant (A) and cell surface expression of the inhibitory molecules PD-L1 or PD-L2 (B) were quantified. Data are presented as box-and-whisker plots with the median value and max/min values illustrated. The Mann-Whitney U test was used for the statistical analysis (* $p < 0.05$ *B. longum* 35624 versus the sEPS^{neg} strain). (C) THP-1 NF- κ B activation following exposure to increasing concentrations of *B. longum* 35624 or its isogenic derivative sEPS^{neg} ($n = 4$ experimental replicates). (D) Activation of NF- κ B in MDDCs exposed to *B. longum* 35624 or its isogenic derivative sEPS^{neg} ($n = 3$, 50 bacteria: 1 MDDC). Statistical significance was determined using two-way ANOVA (* $p < 0.05$ *B. longum* 35624 versus the sEPS^{neg} strain).

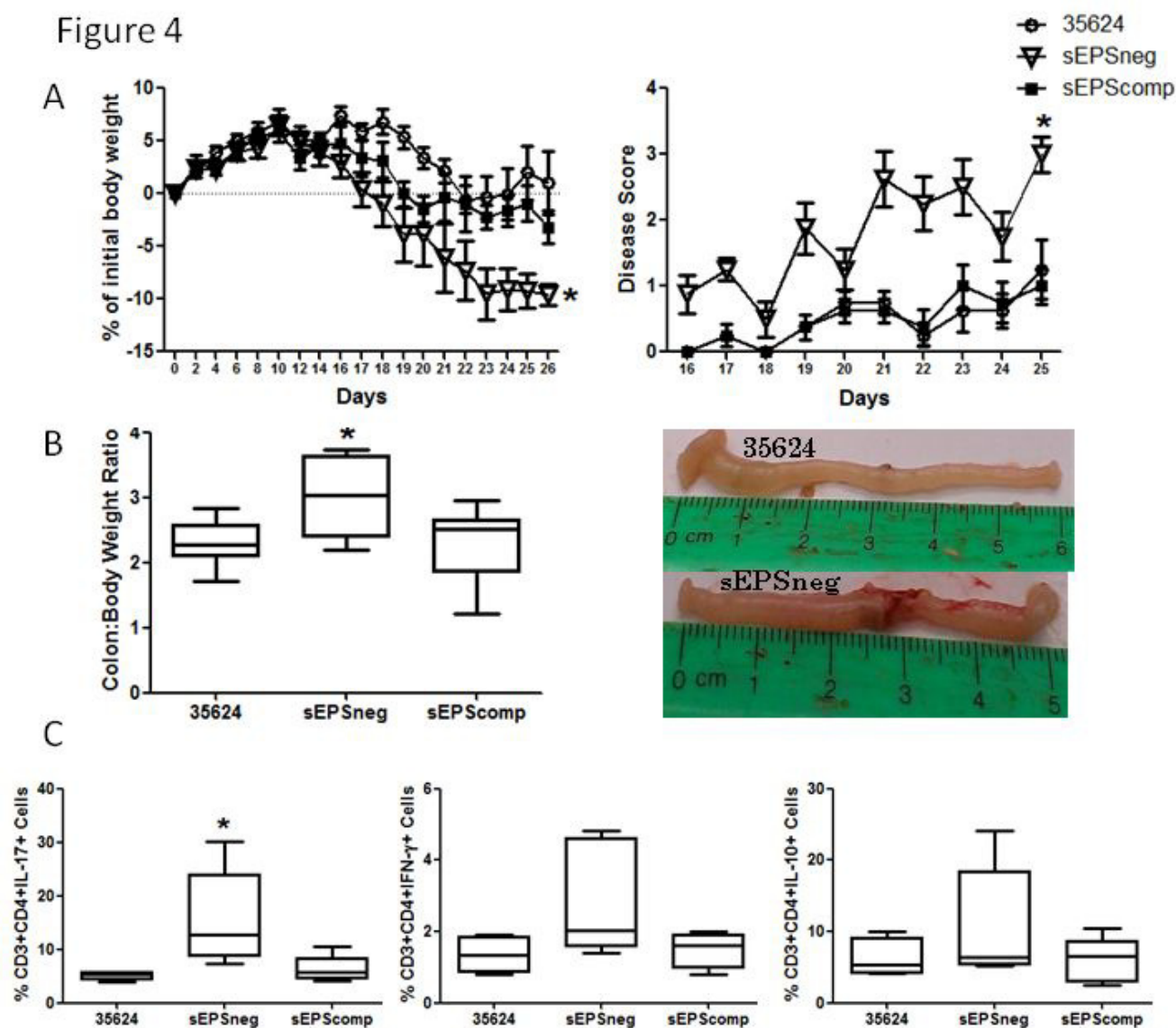
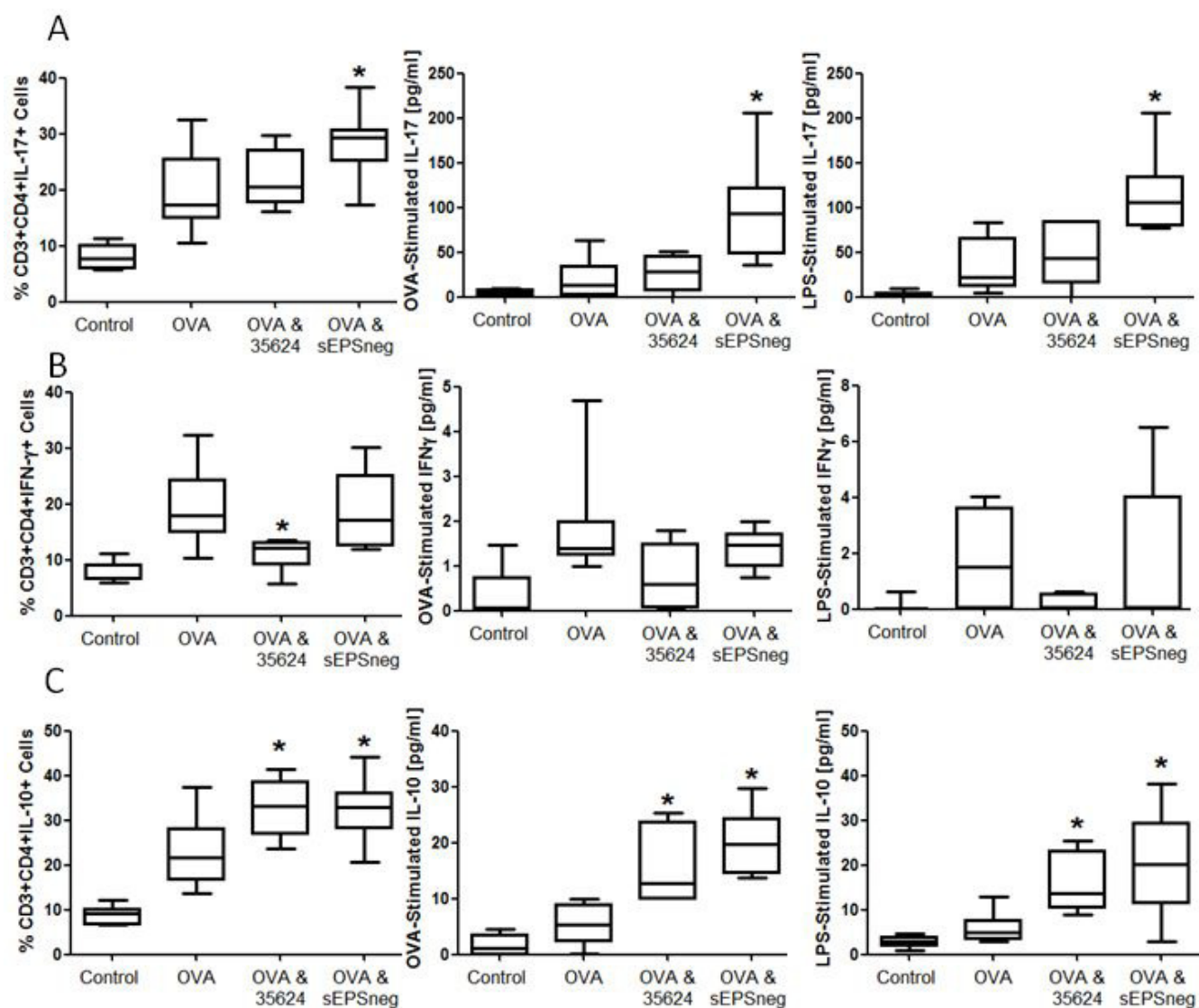


Figure 4. sEPS^{neg} is not protective in a T cell transfer colitis model

Following receipt of CD4⁺CD25⁻CD45RB^{hi} T cells, C.B-17 SCID mice were orally administered *B. longum* 35624 (n=8), sEPS^{comp} (n=8) or sEPS^{neg} (n=8) strains. (A) Weight loss and disease activity were monitored over time. Statistical significance was determined using two-way ANOVA (*p<0.05). (B) Following euthanasia, the colon:body weight ratio was determined. A representative picture of colons from *B. longum* 35624 or sEPS^{neg}-treated animals is provided. (C) The percentage of IL-17⁺, IFN- γ ⁺ and IL-10⁺ lymphocytes from mesenteric lymph nodes are illustrated (n=8 per group). Data are presented as box-and-whisker plots with the median value and max/min values illustrated. Statistical significance was determined using the Kruskal-Wallis test and Dunn's multiple comparison test (*p<0.05 sEPS^{neg} strain versus the other strains).

Figure 5

**Figure 5.** sEPS^{neg} promotes T_H17 responses in the lung

Non-sensitized animals received an OVA aerosol challenge and were intranasally administered PBS (Control, n=8). Sensitized animals received an OVA aerosol challenge and were intranasally administered PBS (OVA, n=8), or intranasally administered *B. longum* 35624 (OVA & 35624, n=8), or intranasally administered sEPS^{neg} (OVA & sEPS^{neg}, n=8). (A) The percentage of IL-17⁺ CD3⁺CD4⁺ T lymphocytes, isolated from lung tissue, and secretion of IL-17 from isolated lung cells re-stimulated *ex vivo* with OVA or LPS. Similarly, IFN- γ ⁺ and IL-10⁺ CD3⁺CD4⁺ T lymphocytes and *ex vivo* IFN- γ and IL-10 secretion were quantified using identical methods, (B) and (C) respectively. Data are presented as box-and-whisker plots with the median value and max/min values illustrated. Statistical significance was determined using the Kruskal-Wallis test and Dunn's multiple comparison test (*p<0.05 compared to the OVA group).